SSRG International Journal of Electrical and Electronics Engineering
ISSN: 2348-8379/ https://doi.org/10.14445/23488379/IJEEE-V13I8P110

Volume 13 Issue 8, 114-125, August 2026

Original Article

Impact of Realistic Voltage Dependent ZIP Load Modeling on Optimal Multi-PV Allocation and Reverse Power Flow Mitigation in Radial Distribution Networks

Rachana J. Patel[1*], Vineeta Chauhan[2], Jayendra Patel[3]

[1,2]*Electrical Engineering Department, Indus University, Ahmedabad, India.*
[3]*Electrical Engineering Department, Government Polytechnic, Ahmedabad, India.*

**Corresponding Author : rjpatel.ee@gmail.com*

Received: 14 June 2026 Revised: 29 July 2026 Accepted: 10 August 2026 Published: 25 August 2026

Abstract - *In the DG integrated modern radial distribution network, for detailed analysis and optimal planning, load representation plays a crucial role. Unlike the traditional constant power load model, the actual distribution load exhibit strong voltage dependency, which can be effectively handled through the ZIP (constant impedance-constant current-constant power) load model. That voltage-dependent load behaviour greatly influences the power flow results, voltage profile and optimal placement and sizing of PVDG, especially when high penetration scenario is considered. This work presents the performance enhancement of IEEE 33 bus system with integration of multiple PVDG when real and experimental ZIP load modelling is incorporated in the distribution network. For optimal size and place selection, two optimization techniques, namely GA and PSO, are implemented, and results are compared to check complexity handling strength of those techniques under the presence of realistic load. Furthermore, the optimization framework included a reverse power flow penalty to restrict power flow in negative direction from load to substation to ensure reliable and safe operation of distribution system with high penetration of PVDGs*.

Keywords - *ZIP load, PQ load, Photovoltaic, Radial distribution network, Reverse Power Flow, Voltage Profile, Loss Reduction, GA, PSO.*

1. Introduction

Distributed Generation (DG) offers environmental and economic benefits at a great level, in addition to guaranteeing technical benefits in the power sector. However, those benefits can't be available if inappropriate sitting and sizing of DG are selected. Due to this reason, the optimal sitting and sizing of Photovoltaic Distributed Generation (PVDG) in radial distribution networks has been an active research area for several decades.

Early research works focused on improving voltage profile and reducing real power losses through network reconfiguration or capacitor placement. But in the last decade, many researchers have proved the extraordinary benefits of DG, in terms of voltage profile improvement and power loss minimization, with the correct implementation of it in the distribution network. In early research work, voltage stability index was used to get information about the weakest bus candidate for DG placement, but recently, several optimization-based techniques have been proposed for determining optimal DG locations and capacities. Gözel and Hocaoglu (2009) presented an analytical sizing and siting method for DG units in radial systems, demonstrating significant loss reduction. Keane and O'Malley (2005) further investigated optimal embedded generation allocation using optimization techniques, highlighting the benefits of DG integration but also noting operational challenges at higher penetration levels. Comprehensive reviews by Georgilakis and Hatziargyriou (2013) and Viral and Khatod (2012) systematically categorized DG placement models, objective functions, and solution techniques, concluding that metaheuristic approaches are particularly effective for solving non-linear DG planning problems. There are many optimization techniques, but some metaheuristic algorithms, such as Genetic Algorithm (GA), Particle Swarm Optimization (PSO), and hybrid methods, have been widely applied for this kind of research due to their ability to handle highly complex problems. Adegoke et al. (2024) demonstrated effective loss minimization and voltage stability enhancement using metaheuristic-based DG placement on standard IEEE test systems. Similarly, Bazrafshan et al. (2019) investigated PV planning under uncertainty with consideration of constant PQ load model and cannot focus on the actual distribution system behavior under voltage variations. But in practical scenario, load modelling is a critical factor in realistic DG planning.

The constant impedance-current-power (ZIP) model better help to represent actual customer load characteristics. Cintuglu et al. (2014) showed that system performance indices, including voltage deviation and losses, vary significantly when ZIP load models are employed instead of constant PQ loads. The IEEE Guide (2022) for Load Modeling and Simulations for Power Systems strongly recommends the use of ZIP or composite load models, particularly in networks with high renewable energy penetration is considered. In the same flow, the issue of Reverse Power Flow (RPF) has also gained increasing attention of researcher and grid operator with high PV penetration levels. Conventional distribution networks were designed for unidirectional power flow, but the modern network with DGs integration, power may have observed bidirectional and this excessive reverse power flow can lead to protection maloperation, voltage regulation issues, and transformer overloading.

Nair and Rajeev (2022) analyzed the impact of high solar PV penetration on distribution protection systems and reported significant reliability concerns under reverse power flow conditions. Majeed and Nwulu (2022) further demonstrated that sustained reverse power flow can accelerate transformer aging and thermal stress in low-voltage networks. Although these studies clearly highlight the severity of RPF, they do not incorporate optimization-based mitigation during the DG planning stage.

Recent studies related to bidirectional power flow, such as electric vehicle integration and active distribution networks, further emphasize the growing complexity of modern distribution systems. Lopes et al. (2011) and Dubey and Santoso (2015) discussed bidirectional power flow impacts on voltage regulation and network operation, reinforcing the need for planning strategies that explicitly account for reverse power flow effects.

1.1. Research Motivation

A majority of DG placement studies neglect voltage-dependent load models and reverse power flow constraints, while RPF-focused studies are largely analytical and do not provide optimal placement and sizing solutions. Moreover, no research simultaneously evaluates all three operating scenarios, like restricted PV penetration, both PQ and ZIP load models, Reverse Power Flow penalty (RPF penalty) within the same optimization framework together. To address these research gaps, this paper presents a GA and PSO-based optimal PV placement and sizing tested on the IEEE 33-bus distribution system. The proposed approach considers both constant PQ and ZIP load models under three distinct PV penetration scenarios, including an explicit reverse power flow penalty to ensure practical and utility-compliant planning.

The key contributions of this work are summarized as follows:

- Development of a multi-objective optimization model considering active power loss minimization and voltage deviation reduction.
- Performance evaluation of GA under identical objective functions and constraint settings.
- Investigation of the impact of PV penetration limits.
- Modeling of reverse power flow using a high penalty-based constraint within the optimization framework.
- Evaluation of optimal PV DG allocation under different load models, including base and ZIP loads, to enhance practical relevance.
- Validation of the proposed approach on the IEEE 33-bus radial distribution system.

2. Problem Statement

2.1. Objective Function

The optimization problem aims to minimize a multi-constrained objective function consisting of total active power loss, voltage deviation and parameter deviation penalty. The proposed multi-objective optimization model aims to minimize the following composite objective function:

$$F = w1 \cdot Ploss + w2 \cdot VD + penalty \qquad (1)$$

Where Ploss denotes the total real power loss in the distribution network, can be calculated from the difference in from and to power of each branch. VD represents the voltage deviation, can be calculated as the sum of absolute deviations of bus voltages (V_i) from the reference value (1 p.u.), which is widely adopted in distribution system optimization studies Equation (2). Here N is the number of bus node.

$$VD = \sum_{i=1}^{N} |V_i - 1| \qquad (2)$$

Deviation Penalty function activated when reverse power flow, voltage limit violence and thermal limit is detected at the substation, discouraging operational violations. Penalty weight for each limit is are discussed in next section. w1, w2 are non-negative weighting coefficients that scale the relative importance of each objective term. The weighting factors are selected based on commonly adopted practices in recent literature. In literature, it has been reported that the weight assigned to active power loss is typically chosen in the range of 0.6-0.8, while the voltage deviation index is assigned a weight in the range of 0.2-0.4 (Rasheed and Verayiah, 2021). These coefficients are tuned with 0.7 and 0.3 for system loss reduction and voltage deviation reduction, respectively, to give primary priority to the minimization of active power loss and secondary priority to reduction of voltage deviation.

2.2. Constraints

The operational constraints considered in this study are essential to ensure the technical feasibility, safety, and practical applicability of the proposed PV-DG planning framework. The optimization problem is subject to the following constraints:

a) Power Balance: PDG + Psubstation = Pload + Ploss
b) Voltage Limits: Vmin ≤ Vi ≤ Vmax, where Vmin is 0.95 p.u and Vmax is 1.05 p.u. (Reddy and Manjula, 2024).
c) Thermal limits: I_line ≤ I_rated
d) PV penetration constraint: ΣPDG ≤ α · Pload, where α is the penetration factor.
e) Reverse power flow constraint: Reverse power flow is penalized when the net power at the substation becomes negative.

The power balance constraint guarantees that the total power injected by the PV-DG units and the substation equals the total system load and network losses, thereby preserving the fundamental law of energy conservation (Wood et al. 2013). The bus voltage limit constraint maintains all node voltages within prescribed limits to ensure acceptable power quality, prevent insulation stress, and avoid under-voltage or over-voltage conditions (IEEE, 2018). Thermal limits constraints can contribute for line safety, and reverse power flow (toward the slack bus) constraints can contribute for utility protection. I_line is the branch current, and I_rated denotes the maximum current-carrying capacity of the branch. It is taken as 5.47 KA, which is 1.2 times of Ibase, where Ibase is calculated from Base MVA and base KV of system under test. A limit of 1.0-1.2 p.u. is widely adopted in literature to ensure safe operation while allowing limited overloading under contingency conditions (Riaz et al. 2024), (Bouali and Alamri, 2025).

Finally, the reverse power flow constraint penalizes operating conditions in which net power at the substation becomes negative, discouraging excessive upstream power injection that can lead to protection maloperation, voltage regulation conflicts, and transformer overloading in traditionally radial distribution networks (Nair and Rajeev, 2022), (Majeed and Nwulu, 2022), (Peças Lopes et al. 2006). Reverse power flow is calculated based on the sign of active power flow in each branch obtained from load flow results. A negative value of active power flow in line (Pij) indicates that the direction of power flow is reversed, i.e., power flows from the receiving end back toward the source. Therefore, reverse power flow is quantified as the summation of the magnitudes of all negative branch power flows, as shown in Equation (3):

$$P_{reverse} = \sum_{i=1}^{N} |P_{ij}| \qquad for\ P_{ij} < 0 \tag{3}$$

The constraints are incorporated using penalty weights within the optimization framework. Penalty weights are selected based on the severity of constraint violations. A large penalty factor ensures that any violation of operational constraints significantly increases the fitness value, thereby discouraging infeasible solutions and guiding the optimization algorithm toward feasible and practically acceptable operating conditions.

3. Optimization Technique

Genetic Algorithm (GA) is a population-based evolutionary optimization technique inspired by natural selection and genetic inheritance, and its ability to effectively handle mixed discrete-continuous variables and complex search spaces, it has been widely applied in power system optimization (Afshar Bali et al. 2019), (Abasi and Karbalaei, 2013). The general structure of GA is shown in Algorithm 1. Particle Swarm Optimization (PSO) is a population-based metaheuristic optimization technique inspired by the social behavior of bird flocking and fish schooling. PSO has been extensively used for optimal placement and sizing selection of PVDG-related complex and nonlinear problem due to its simple implementation, fast convergence characteristic (Freitas et al. 2020). The general structure of PSO is shown in Algorithm 2.

Algorithm 1. The structure of genetic algorithm.

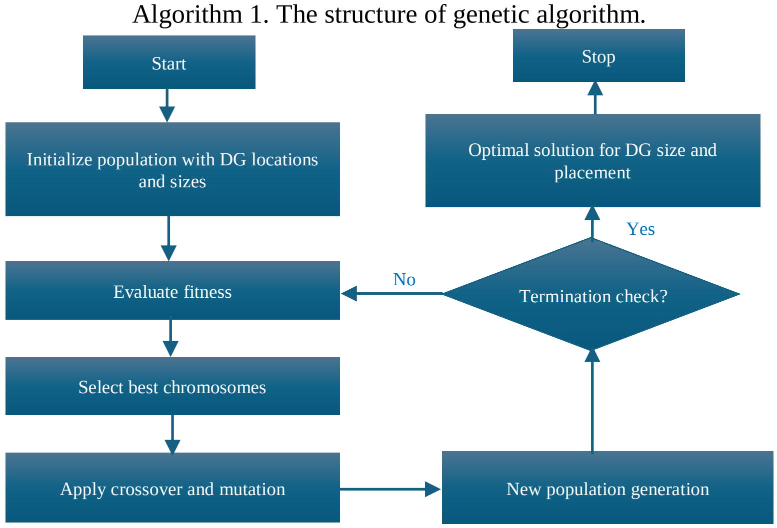

Each optimization was performed using a population size of 50 and 100 maximum iterations. For PSO, inertia weight was varied from 0.9 to 0.4, while both cognitive and social coefficients (c1 and c2) were set to 2 for balanced exploration and exploitation during the optimization process.

Algorithm 2. The structure of particle swarm optimization.

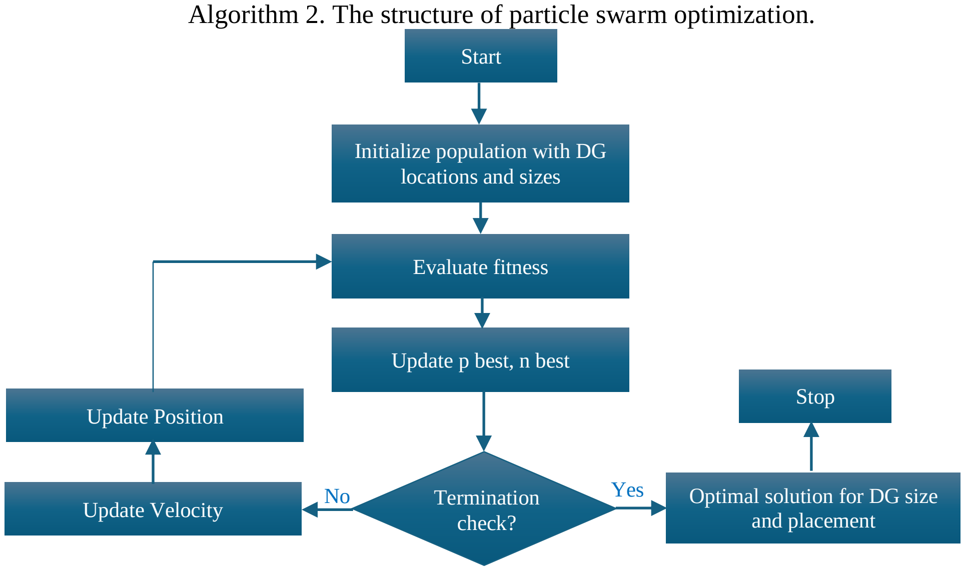

4. Test System

Baran and Wu (1989) introduced one of the most widely used RDN test systems, which later became the basis for DG and PV integration studies. System (base) is with a total connected load of 3.715 MW and 2.3 MVAR distributed across 33 buses. The system consists of 32 branches connecting the 33 buses, with individual bus loads varying from 45 kW/30 kVAR to 420 kW/200 kVAR. Bus 1 serves as the substation (slack bus), supplying power to the network. The system configuration is shown in Figure 1.

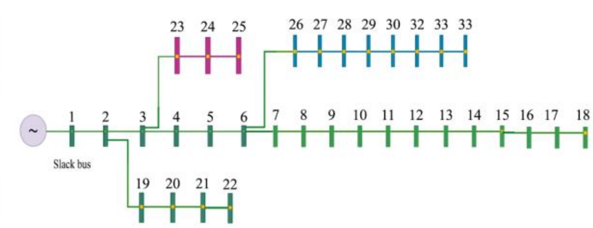

Fig. 1 IEEE 33 bus system

Such a relatively small system, with uneven load distribution and radial network topology, is a common system used as a benchmark system to test PV placement and sizing and optimization algorithms.

5. ZIP Load Model

These days, researchers are really diving into considering various loading conditions to ensure precise power system analysis. Afshar Bali et al. (2019) came up with a novel hybrid load modeling approach that combines ZIP and induction motor components, all optimized using PSO. They showed that having an accurate load representation can really enhance load-flow results. Abasi and Karbalaei (2013) took a look at voltage-dependent load models in PV curve analysis and discovered that these loads decrease the stability margin compared to constant power models. In order to enhance the practical relevance of this study, ZIP load model have been incorporated. The ZIP load model effectively encompasses load demand as a combination of constant impedance (Z), constant current (I), and constant power (P) elements, enabling a much more precise depiction of voltage-dependent load traits. The ZIP load model can be mathematically expressed as mentioned in Equations (4) and (5).

$$P = P_o \cdot \left[a_z \cdot \left(\frac{V}{V_o}\right)^2 + a_i \cdot \left(\frac{V}{V_o}\right) + a_p \right] \tag{4}$$

$$Q = Q_o \cdot \left[b_z \cdot \left(\frac{V}{V_o}\right)^2 + b_i \cdot \left(\frac{V}{V_o}\right) + b_p \right] \tag{5}$$

Here, a_z, a_i, and a_p represent the ZIP coefficients of active power, while b_z, b_i, and b_p represent the ZIP coefficients of reactive power corresponding to constant impedance, constant current, and constant power components, respectively. These coefficients satisfy the conditions given in Equation (6).

$$\left.\begin{aligned} a_z + a_i + a_p &= 1 \\ b_z + b_i + b_p &= 1 \end{aligned}\right\} \tag{6}$$

ZIP load distribution across IEEE 33-Bus System and experimental weight coefficients used in the study for active power (P) and reactive power (Q) are given in Table 1 (Parker et al. (2021)). The bus numbers where such loads are implemented for this study are shown in Table 2. Such realistic load representation helps to understand actual behavior of radial distribution system.

Table 1. Weight coefficients of ZIP load model from experimental data

Load Type	a - Coefficients for (P) [ZIP]	b - Coefficients for (Q) [ZIP]
Constant Power Load (P-type)	[1.83, -1.66, 0.83]	[1.87, -1.83, 0.96]
Constant Current Load (I-type)	[0.00, 1.66, -0.63]	[0.00, 1.66, -0.63]
Constant Impedance Load (Z-type)	[0.87, 0.12, 0.00]	[0.87, 0.12, 0.00]

Table 2. Distribution of ZIP load on selected bus number

Load Type	Selected Bus Numbers
Constant Power Load (P-type)	3, 4, 7, 10, 11, 15, 17, 20, 24, 27, 29
Constant Current Load (I-type)	3, 4, 7, 10, 11, 15, 17, 20, 24, 27, 29
Constant Impedance Load (Z-type)	2, 6, 9, 14, 18, 21, 23, 26, 28, 31, 33

6. Simulation Results

As a First step, load flow analysis is carried out for IEEE 33 bus system with ZIP load, and results are compared with PQ load-based system results. Table 3 shows the difference that helps to examine the influence of load characteristics on system performance. Unlike the constant PQ model, the ZIP model allows part of the load demand to vary with bus voltage magnitude. Voltage drops in a feeder result in the decrement of actual power consumption, which reduce the feeder current and hence reduce the active power loss and improve the voltage profile.

Table 3. Base case results with PQ and ZIP load

Load Model	Base case results
Constant PQ load	Active power loss- 202.6771 kW Min Voltage = 0.9131 pu on bus 18
ZIP load	Active power loss = 164.5646 kW Min Voltage = 0.9229 pu on bus 18

Further analysis was carried out to investigate the impact of different Photovoltaic (PV) penetration levels, i.e 100%, 70% and 50% penetration, on reverse power flow in the IEEE 33-bus radial distribution network. For optimal placement and sizing of single PV, GA and PSO algorithms are applied. Initially, the study was performed using the conventional PQ load model, and the obtained results were subsequently compared with those obtained using the voltage-dependent ZIP load model.

Figures 2,3 and 4 shows the branch current when single PV was integrated with PQ load-based system at 100%, 70% and 50 % penetration level respectively. Those results demonstrate that the more total reverse power flow is observed when PV penetration was maximum.

The restricted penetration strategy surely helps to reduce the total reverse power flow, but cannot eliminate that completely. In Figure 4, at 50% PV penetration, less total reverse power flow is observed compare to 70% and 100% PV penetration (Figures 2 and 3), but not zero. The same can be observed from Figure 5 with numerical values of observed total reverse power flow at various PV penetration level under the consideration of PQ load.

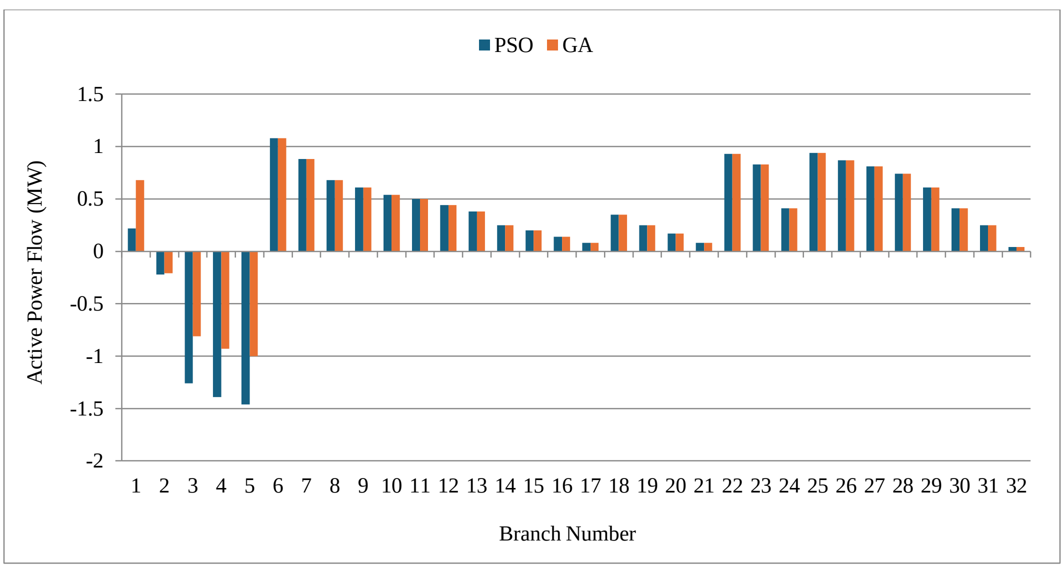

Fig. 2 Branch current with 100% penetration of 1 PV (PQ load)

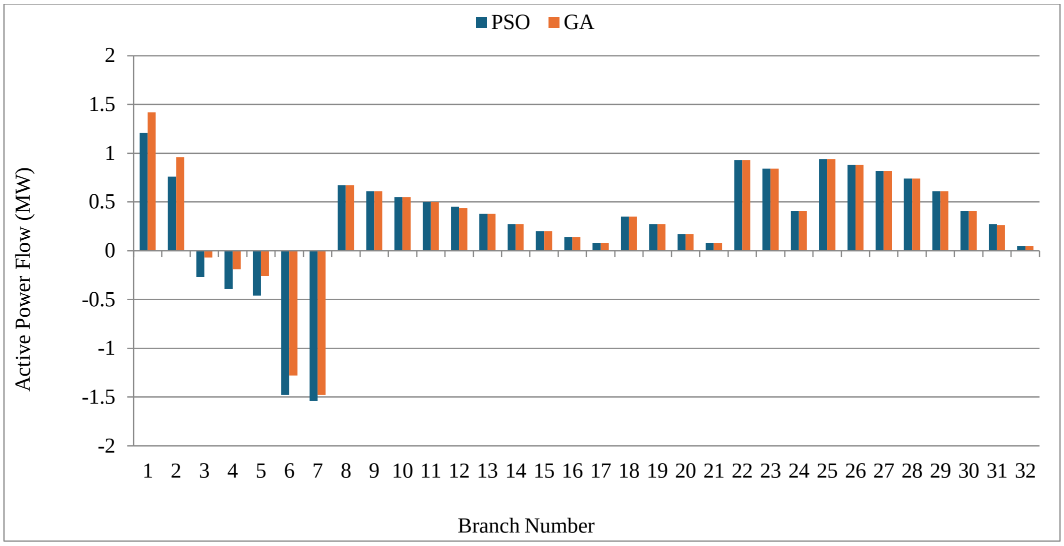

Fig. 3 Branch current with 70 % penetration of 1 PV (PQ load)

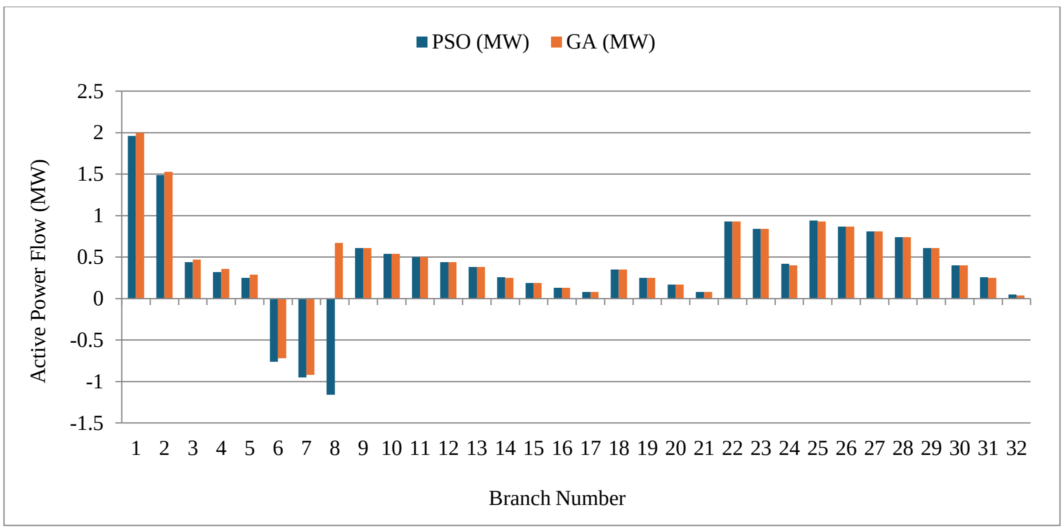

Fig. 4 Branch current with 50 % penetration of 1 PV (PQ load)

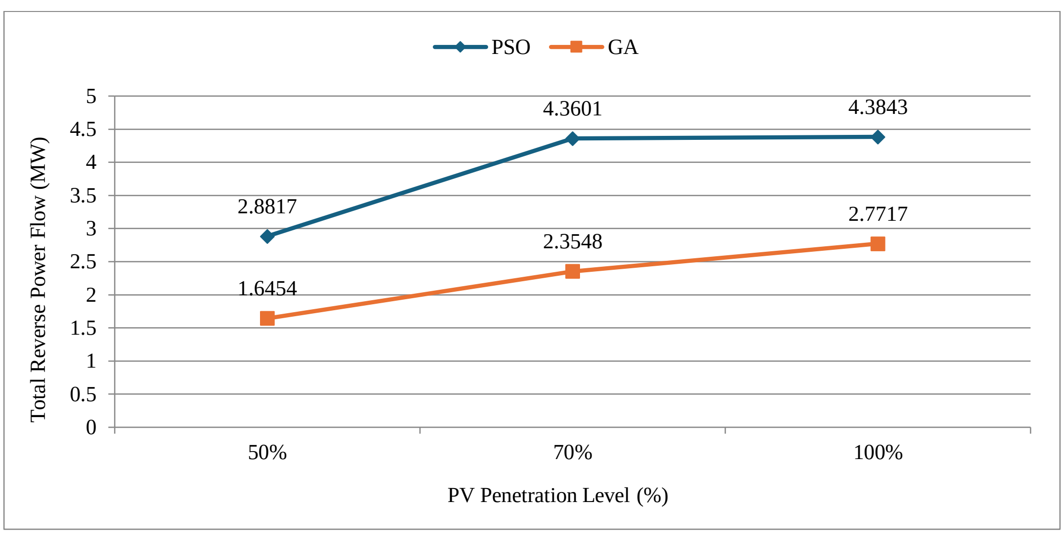

Fig. 5 PV penetration level vs total reverse power flow in MW (1 PV, PQ load)

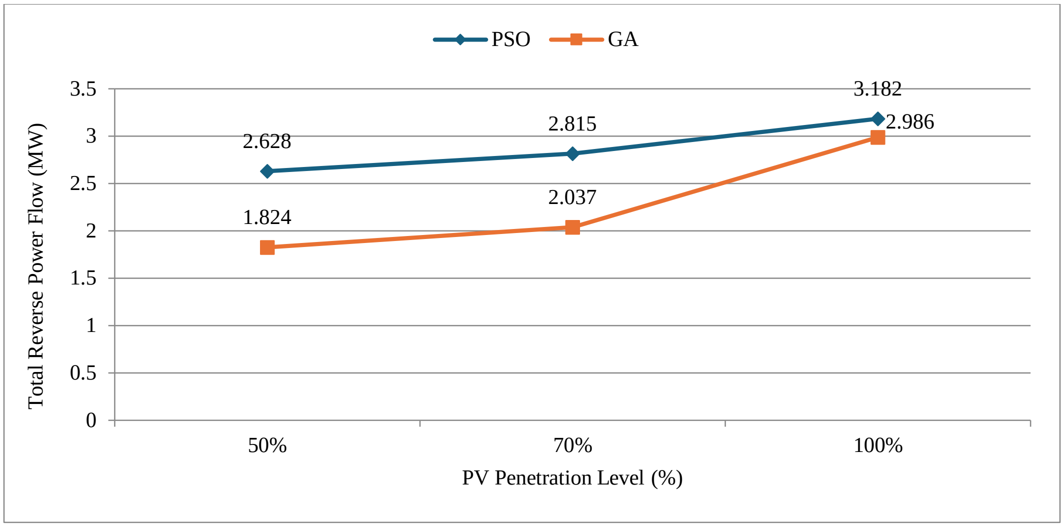

Fig. 6 PV penetration level vs total reverse power flow in MW (1 PV, ZIP load)

The results in Figures 5 and 6 indicate that reverse power flow increases with higher PV penetration levels in both load models. However, the magnitude of reverse power flow observed in the ZIP load model is comparatively lower than that obtained with the PQ load model. ZIP load model led to better local utilization of generated PV power, thereby reducing the amount of surplus power flowing back toward the substation. In contrast, the PQ load model assumes constant power demand irrespective of voltage variations, which tends to overestimate reverse power flow under high PV penetration conditions. These findings highlight the importance of voltage dependent ZIP load model consideration for accurate analysis of reverse power flow after PV penetration in a radial distribution network.

To further evaluate the influence of load modeling on photovoltaic distributed generation planning, the optimal placement and sizing of PV units were investigated under both PQ and ZIP load models for single-PV and multi-PV scenarios. The obtained results demonstrate that the selected bus locations and optimal PV sizes vary depending on the adopted load model. From all previous results, one can observed the behavior of voltage independent PQ load and voltage dependent ZIP load in term of branch current, active power loss, reverse power flow and minimum voltage value. Due to this performance variation of both load model, in ZIP load, the buses identified as optimal for PV installation and the corresponding PV capacities are differ from those obtained using the PQ load model. Table 4 shows the bus and size selection of single and multi-PV in both load model. In the case of 1 PV, same optimal bus location is selected by PSO and GA for both load model. But the size selection is differed. The slight variation in PV size obtained using PSO and GA is mainly due to differences in the search mechanism and convergence characteristics of the optimization algorithms. PSO generally provides faster convergence toward the global optimum through collective particle movement, whereas GA relies on crossover and mutation operations that may lead to slightly different near-optimal solutions. The optimal PV size obtained using the ZIP load model is lower than that obtained with the PQ load model, and same can be observed for multi-PV scenarios.

Table 4. Bus and size (in MW) selection with 100% penetration without RPF penalty

Load Model	Tool	1 PV	2 PV	3 PV
PQ load	PSO	6, 3.599	13, 1.224 30, 1.536	31, 0.889 14, 0.878 6, 1.697
	GA	6, 3.131	26, 2.495 13, 0.971	15, 0.881 8, 1.571 23, 1.018
ZIP load	PSO	6, 3.124	13, 1.127 29, 1.441	24, 1.245 30, 1.245 13, 1.091
	GA	6, 3.096	28, 1.493 14, 1.043	26, 1.277 24, 0.737 13, 1.362

In the PQ load model, the load demand remains constant regardless of voltage magnitude, resulting in comparatively higher feeder current and active power losses. Consequently, a larger PV size is required to compensate for these losses and improve the voltage profile. In contrast, the voltage-dependent ZIP load behavior naturally reduces feeder current, active power loss, and reactive power burden on the system. As a result, a comparatively smaller PV capacity becomes sufficient to achieve the desired loss minimization and voltage improvement objectives. Overall, the results demonstrate that voltage-dependent ZIP load modeling significantly influences the optimal sizing of PV units and provides a more realistic representation for distributed generation planning studies.

Further investigation was carried out to analyze the effect of single and multiple PV installations on total reverse power flow under both PQ and ZIP load models. The results are shown in Table 5. The obtained results show that as the number of PV units and PV penetration level increase from single-PV to multi-PV scenarios, the total reverse power flow in the distribution network also increases. On other side higher number of distributed PV generation supplies a larger portion of local load demand, hence provide better loss reduction and better voltage profile.

Table 5. Reverse power flow (MW) with 100% penetration without RPF penalty

Load Model	Tool	1 PV	2 PV	3 PV
PQ load	PSO	4.384	9.041	6.948
	GA	2.772	7.549	6.511
ZIP load	PSO	2.986	5.851	6.685
	GA	3.182	5.445	6.526

Results given in Table 6 highlights that effect clearly. But during certain operating conditions, the generated power exceeds the local consumption, causing surplus power to flow back toward the upstream network or substation. This issue highlights the need of incorporating reverse power flow penalty as an important constraints in the optimization framework.

Table 6. % loss reduction without RPF

Load Model	Tool	1 PV	2 PV	3 PV
PQ load	PSO	41.76%	50.54 %	54.39%
	GA	41.64 %	47.29 %	50.30%
ZIP load	PSO	37.57 %	44.33%	52.09%
	GA	36.66 %	43.19 %	43.31%

Such kind of excessive RPF can create operational challenges such as voltage rise, protection coordination issues, and reduced network stability. Therefore, adding the RPF penalty enables the optimization algorithm to achieve a balanced solution that minimizes power losses while maintaining secure and reliable distribution system operation.

The ZIP load model makes the load flow behavior more dynamic and computationally challenging. Furthermore, the addition of heavily penalized RPF constraints forces the optimization algorithms to simultaneously minimize losses, improve voltage profile, and restrict excessive upstream power injection.

The comparison of optimal PV allocation results before (Table 4) and after (Table 7) incorporating reverse power flow penalty shows that not only the PV sizes but also the selected bus locations change significantly in most cases. Without RPF consideration, the optimization algorithms mainly prioritize buses that provide maximum loss reduction and voltage improvement, often resulting in larger PV capacities concentrated at a few highly sensitive buses.

However, after introducing the RPF penalty, the optimization framework must additionally control excessive upstream power injection and voltage rise. Consequently, the algorithms shift PV placement toward different bus combinations where locally generated power can be more effectively consumed by nearby loads, thereby reducing reverse power flow. This results in the redistribution of PV units across the network, along with reduced PV capacities.

Table 7. Bus and size (in MW) selection with 100% penetration with RPF penalty

Load Model	Tool	1 PV	2 PV	3 PV
PQ load	PSO	6, 2.115	10, 0.618 6, 1.486	30, 0.196 3, 1.248 6, 1.898
	GA	6, 2.063	24, 0.688 7, 1.026	7, 0.870 3, 2.704 19, 0.200
ZIP load	PSO	6, 1.981	13, 0.415 29, 0.698	32, 0.112 6, 1.877 24, 0.694
	GA	6,1.813	19, 0.395 6, 1.894	7, 0.874 23,0.9512 4, 1.024

The variation in bus selection becomes more prominent in multi-PV scenarios because the optimization problem becomes highly nonlinear and multi-dimensional.

Table 8. % loss reduction with RPF

Load Model	Tool	1 PV	2 PV	3 PV
PQ load	PSO	47.24 %	52.75 %	53.46 %
	GA	46.88 %	50.36 %	51.64 %
ZIP load	PSO	41.84 %	42.51 %	50.25 %
	GA	40.79 %	41.84 %	41.99 %

For PQ load model, the inclusion of the RPF penalty improves the obtained loss reduction (Table 8) compare to the loss reduction results obtained without inclusion of RPF penalty (Table 6). However, the behavior under the ZIP load model is different. Since the ZIP load model already exhibits voltage-dependent characteristics, the base-case feeder current and active power losses are inherently lower than those of the PQ load model. Consequently, after adding the RPF penalty, the optimization process becomes more restrictive because it must simultaneously satisfy voltage-dependent load behavior and reverse power flow limitations. Under higher PV penetration levels, this forces the algorithm to reduce PV capacities or shift PV locations to maintain acceptable RPF levels, thereby limiting the achievable loss reduction. These observations confirm that realistic load modeling and reverse power flow constraints have a major impact overall performance of renewable source integrated radial distribution systems.

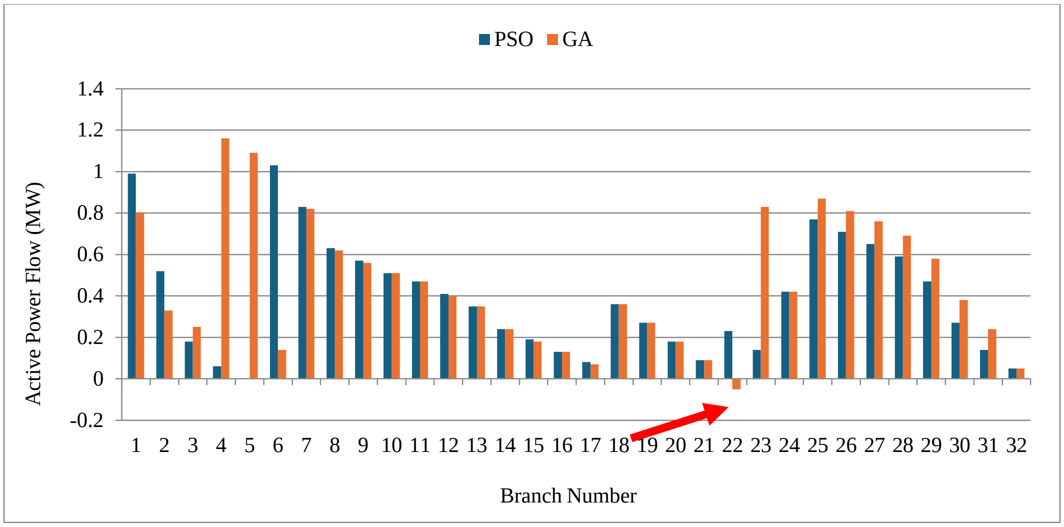

Fig. 7 Branch current with maximum penetration of 3 PV (ZIP load) with RPF penalty (30 KW power in reverse with GA)

One important takeaway from Table 8 is related to GA and PSO performance. The results indicate that PSO performs more effectively than GA, particularly in the three-PV case under the ZIP load model with reverse power flow constraints. The inclusion of voltage-dependent ZIP loads and heavily penalized RPF constraints makes the optimization problem highly nonlinear, multi-dimensional, and strongly constrained.

Under such complex operating conditions, PSO demonstrates better convergence capability and global search performance, enabling it to obtain more balanced PV allocation with higher loss reduction. In contrast, GA performance slightly degrades due to its dependence on crossover and mutation operations, which may lead to slower convergence and premature trapping in local optimal solutions under highly constrained search spaces. Figure 7 shows the branch current when 3 PVs are integrated under the ZIP load consideration. It can be clearly observed that even with RPF constraints, GA provide size and location of 3 PVs, which still provide a small amount of reverse power at branch number 22. This highlights the poor strength of GA to handle highly complex, multi-dimensional and nonlinear problem. On other side, PSO appears more suitable for solving such complex PV allocation problems involving ZIP load modeling and reverse power flow limitations. The outstanding performance of PSO over GA can be further conformed by means of the convergence graph and voltage profile graph when 3 PVs are integrated with inclusion of RPF penalty for PQ and ZIP load model. Figure 8 represents the voltage profile with ZIP load model, and Figure 9 represents the voltage profile with PQ load model. In both the case, PSO helps better over GA to provide improved voltage profile, especially at the far-end buses. Also, all the bus voltages are above the 0.95 pu (threshold value).

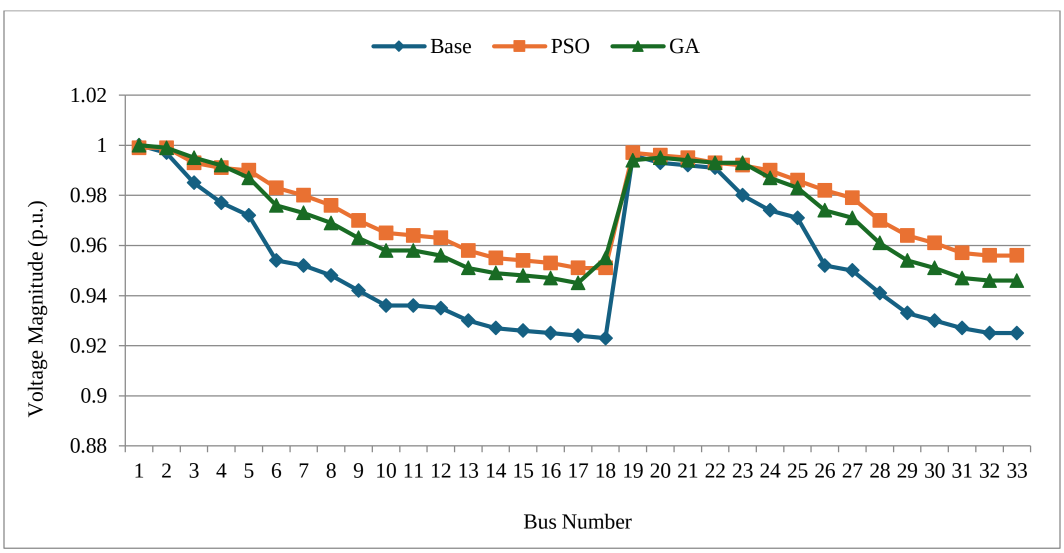

Fig. 8 Voltage profile when 3 PV installed with ZIP load model when RPF penalty is applied

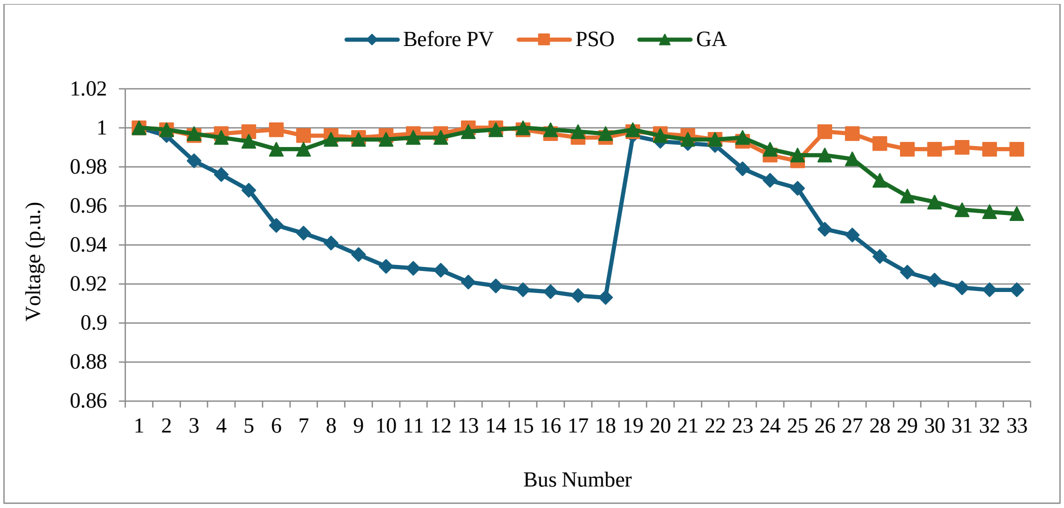

Fig. 9 Voltage profile when 3 PV installed with PQ load when RPF penalty is applied.

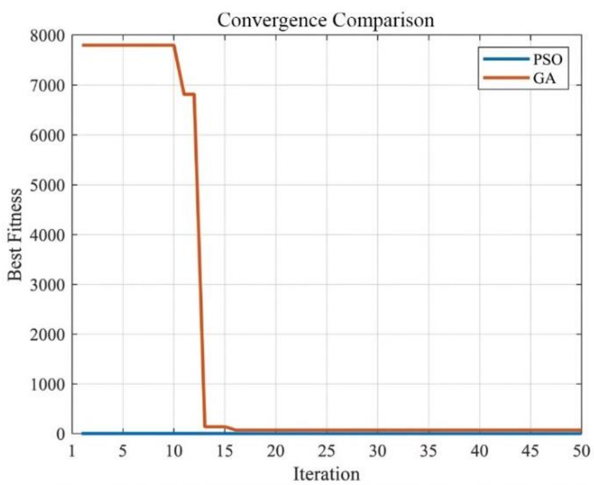

Fig.10 Convergence graph when 3 PV installed with ZIP load

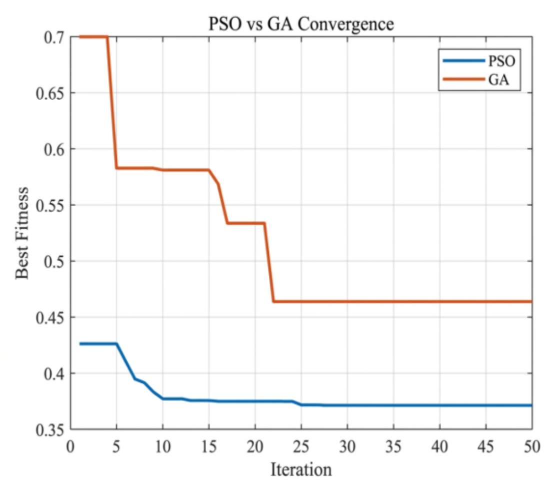

Fig. 11 Convergence graph when 3 PV installed with PQ load

Figures 8 and 9 states that after optimal placement and sizing of three PV units, all bus voltages in the ZIP load-based distribution network remain above 0.98 pu, whereas the minimum bus voltage under the PQ load model is approximately 0.95 pu. It means the injected PV power provides more effective voltage support throughout the distribution network under the ZIP load consideration.

7. Conclusion

This study investigated optimal multi-PV placement and sizing in radial distribution networks under PQ and ZIP load models while incorporating Reverse Power Flow (RPF) constraints into the optimization framework. The results indicate that studies based solely on the conventional PQ load assumption may underestimate the voltage support capability of distributed PV systems. Incorporating voltage-dependent ZIP load characteristics provides a more realistic assessment of PV hosting capacity and network voltage regulation performance. The results further revealed that restricting PV penetration can reduce RPF; however, it is insufficient to eliminate it completely under high PV penetration levels. The inclusion of an RPF penalty effectively mitigated reverse power flow and ensured secure network operation.

Importantly, despite the additional RPF constraint, the network was still able to achieve considerable active power loss reduction, indicating that reverse power flow mitigation can be accomplished without significantly compromising the technical benefits of PV integration. A comparative evaluation of PSO and GA showed that PSO consistently outperformed GA in terms of active power loss reduction, voltage profile improvement, convergence behavior, and its ability to handle the highly nonlinear and multidimensional optimization problem associated with multi-PV planning under strict RPF constraints.

Conflicts of Interest

There is no known conflict of interest associated with the research work mentioned in the paper. The study in the paper was carried out independently.

References

[1] Tuba Gözel, and M. Hakan Hocaoglu, "An Analytical Method for the Sizing and Siting of Distributed Generators in Radial Systems," *Electric Power Systems Research*, vol. 79, no. 6, pp. 912-918, 2009. [CrossRef] [Google Scholar] [Publisher Link]

[2] A. Keane, and M. O'Malley, "Optimal Allocation of Embedded Generation on Distribution Networks," *IEEE Transactions on Power Systems*, vol. 20, no. 3, pp. 1640-1646, 2005. [CrossRef] [Google Scholar] [Publisher Link]

[3] Pavlos S. Georgilakis, and Nikos D. Hatziargyriou, "Optimal Distributed Generation Placement in power Distribution Networks: Models, Methods, and Future Research," *IEEE Transactions on Power Systems*, vol. 28, no. 3, pp. 3420-3428, 2013. [CrossRef] [Google Scholar] [Publisher Link]

[4] Rajkumar Viral, and D.K. Khatod, "Optimal Planning of Distributed Generation Systems in Distribution System: A Review," *Renewable and Sustainable Energy Reviews*, vol. 16, no. 7, pp. 5146-5165, 2012. [CrossRef] [Google Scholar] [Publisher Link]

[5] Samson Ademola Adegoke et al., "Optimal Placement of Distributed Generation to Minimize Power Loss and Improve Voltage Stability," *Heliyon*, vol. 10, no. 21, pp. 1-28, 2024. [CrossRef] [Google Scholar] [Publisher Link]

[6] Mohammadhafez Bazrafshan et al., "Stochastic Planning of Distributed Photovoltaic Generation," *Energies*, vol. 12, no. 3, pp. 1-20, 2019. [CrossRef] [Google Scholar] [Publisher Link]

[7] Mehmet H. Cintuglu, Armando Altamirano, and Osama A. Mohammed, "Modeling of PV based Distributed Generator Systems with Diverse Load Patterns," *The 12th Latin American and Caribbean Conference for Engineering and Technology*, Miami, pp. 1-10, 2014. [Google Scholar]

[8] IEEE Standards Association, IEEE Std 2781-2022, IEEE Guide for Load Modeling and Simulations for Power Systems, 2022. [Online]. Available: https://standards.ieee.org/ieee/2781/7317/

[9] Divya S. Nair, and T. Rajeev, "Impact of Reverse Power Flow due to High Solar PV Penetration on Distribution Protection System," *Sustainable Energy and Technological Advancements*, Singapore: Springer, pp. 1-13, 2022. [CrossRef] [Google Scholar] [Publisher Link]

[10] Issah Babatunde Majeed, and Nnamdi I. Nwulu, "Impact of Reverse Power Flow on Distributed Transformers in a Solar-Photovoltaic-Integrated Low-Voltage Network," *Energies*, vol. 15, no. 23, pp. 1-19, 2022. [CrossRef] [Google Scholar] [Publisher Link]

[11] João A. Peças Lopes, Filipe Joel Soares, and Pedro M. Rocha Almeida, "Integration of Electric Vehicles in the Electric Power System," *Proceedings of the IEEE*, vol. 99, no. 1, pp. 168-183, 2011. [CrossRef] [Google Scholar] [Publisher Link]

[12] Anamika Dubey, and Surya Santoso, "Electric Vehicle Charging on Residential Distribution Systems: Impacts and Mitigations," *IEEE Access*, vol. 3, pp. 1871-1893, 2015. [CrossRef] [Google Scholar] [Publisher Link]

[13] Mohamed Abdul Rasheed, and Renuga Verayiah, "Investigation of Optimal PV Allocation to Minimize System Losses and Improve Voltage Stability for Distribution and Transmission Networks using MATLAB and DigSilent" *Frontiers in Energy Research*, vol. 9, pp. 1-13, 2021. [CrossRef] [Google Scholar] [Publisher Link]

[14] Simarla Vijender Reddy, and M. Manjula, "Performance of the Distribution Network by Connecting Solar and Wind DGs," *Renewable Energy Focus*, vol. 48, pp. 1-14, 2024. [CrossRef] [Google Scholar] [Publisher Link]

[15] Allen J. Wood, Bruce F. Wollenberg, and Gerald B. Sheblé, *Problem Solutions for Power Generation, Operation, and Control*, 3rd ed., Wiley, 2013. [Publisher Link]

[16] "1547-2018 IEEE Standard for Interconnection and Interoperability of Distributed Energy Resources with Associated Electric Power Systems Interfaces," *IEEE*, pp. 1-138, 2018. [CrossRef] [Google Scholar] [Publisher Link]

[17] Muhammad Usman Riaz et al., "Advanced Energy Management in a Sustainable Integrated Energy System," *Energies*, vol. 17, no. 20, pp. 1-53, 2024. [CrossRef] [Google Scholar] [Publisher Link]

[18] Yacine Bouali, and Basem Alamri, "Enhancing Radial Distribution System Performance through Optimal Allocation and Sizing of Photovoltaic and Wind Turbine Distribution Generation Units with Rüppell's Fox Optimizer," *Mathematics*, vol. 13, no. 15, pp. 1-34, 2025. [CrossRef] [Google Scholar] [Publisher Link]

[19] J.A.P. Lopes, C.L. Moreira, and A.G. Madureira, "Defining Control Strategies for Microgrids Islanded Operation," *IEEE Transactions on Power Systems*, vol. 21, no. 2, pp. 916-924, 2006. [CrossRef] [Google Scholar] [Publisher Link]

[20] Ahmed A. Zaki Diab, Ashraf M. Abdelhamid, and Hamdy M. Sultan, "Comprehensive Analysis of Optimal Power Flow using Recent Metaheuristic Algorithms," *Scientific Reports*, vol. 14, no. 1, pp. 1-62, 2024. [CrossRef] [Google Scholar] [Publisher Link]

[21] M.E. Baran, and F.F. Wu, "Optimal Capacitor Placement on Radial Distribution Systems," *IEEE Transactions on Power Delivery*, vol. 4, no. 1, pp. 725-734, 1989. [CrossRef] [Google Scholar] [Publisher Link]

[22] Afshar Bali et al., "Load Modeling based on Real Data Applying PSO Algorithm," *MAJLESI Journal of Electrical Engineering*, vol. 13, no. 3, pp. 15-25, 2019. [Google Scholar]

[23] Shahriar Abasi, and Farid Karbalaei, "Quadratic Approximation of PV Curve Path based on Local Phasor Measurements, in Presence of Voltage Dependent Loads," *MAJLESI Journal of Electrical Engineering*, vol. 7, no. 3, pp. 8-13, 2013. [Google Scholar] [Publisher Link]

[24] Diogo Freitas, Luiz Guerreiro Lopes, and Fernando Morgado-Dias, "Particle Swarm Optimisation: A Historical Review Up to the Current Developments," *Entropy*, vol. 22, no. 3, pp. 1-36, 2020. [CrossRef] [Google Scholar] [Publisher Link]

[25] Andrew Parker et al., "Framework to Develop Time- and Voltage-Dependent Building Load Profiles using Polynomial Load Models," *IEEE Access*, vol. 9, pp. 128328-128344, 2021. [CrossRef] [Google Scholar] [Publisher Link]

[26] Abdullah Bokhari et al., "Experimental Determination of the ZIP Coefficients for Modern Residential, Commercial, and Industrial Loads," *IEEE Transactions on Power Delivery*, vol. 29, no. 3, pp. 1372-1381, 2014. [CrossRef] [Google Scholar] [Publisher Link]

[27] Aditya Karnik, "*Performance of TCP Congestion Control with Rate Feedback: TCP/ABR and Rate-Adaptive TCP/IP*," M.E. Thesis, Indian Institute of Science, Bangalore, India, 1999. [Google Scholar]

[28] Jitendra Padhye, Victor Firoiu, and Don Towsley, "*A Stochastic Model of TCP Reno Congestion Avoidance and Control*," University of Massachusetts, US, 1999. [Google Scholar] [Publisher Link]

[29] 802.11-2020 - IEEE Standard for Information Technology--Telecommunications and Information Exchange between Systems - Local and Metropolitan Area Networks--Specific Requirements - Part 11: Wireless LAN Medium Access Control (MAC) and Physical Layer (PHY) Specifications, *IEEE*, pp. 1-4379, 2021. [CrossRef] [Google Scholar] [Publisher Link]